What is all this fuss about Tus?

Comparison of recent findings from biophysical and biochemical experiments

Berghuis, Bojk; Raducanu, Vlad-Stefan; Elshenawy, Mohamed M.; Jergic, Slobodan; Depken, Martin; Dixon, NE; Hamdan, Samir M.; Dekker, Nynke

DOI
10.1080/10409238.2017.1394264

Publication date
2017

Document Version
Final published version

Published in
Critical Reviews in Biochemistry and Molecular Biology

Citation (APA)
Berghuis, B., Raducanu, V.-S., Elshenawy, M. M., Jergic, S., Depken, M., Dixon, NE., Hamdan, S. M., & Dekker, N. (2017). What is all this fuss about Tus? Comparison of recent findings from biophysical and biochemical experiments. *Critical Reviews in Biochemistry and Molecular Biology*, 1-15. https://doi.org/10.1080/10409238.2017.1394264

CRITICAL REVIEWS IN BIOCHEMISTRY AND MOLECULAR BIOLOGY, 2017
https://doi.org/10.1080/10409238.2017.1394264

Taylor & Francis
Taylor & Francis Group

REVIEW ARTICLE

OPEN ACCESS Check for updates

What is all this fuss about Tus? Comparison of recent findings from biophysical and biochemical experiments

Bojk A. Berghuis[a]*, Vlad-Stefan Raducanu[b], Mohamed M. Elshenawy[b]†, Slobodan Jergic[c], Martin Depken[a], Nicholas E. Dixon[c], Samir M. Hamdan[b] and Nynke H. Dekker[a]

[a]Department of Bionanoscience, Kavli institute of Nanoscience, Delft University of Technology, Delft, the Netherlands; [b]Division of Biological and Environmental Science and Engineering, King Abdullah University of Science and Technology, Thuwal, Saudi Arabia; [c]Centre for Medical and Molecular Bioscience, University of Wollongong, Wollongong, New South Wales, Australia

ABSTRACT

Synchronizing the convergence of the two-oppositely moving DNA replication machineries at specific termination sites is a tightly coordinated process in bacteria. In *Escherichia coli*, a "replication fork trap" – found within a chromosomal region where forks are allowed to enter but not leave – is set by the protein–DNA roadblock Tus–*Ter*. The exact sequence of events by which Tus–*Ter* blocks replisomes approaching from one direction but not the other has been the subject of controversy for many decades. Specific protein–protein interactions between the nonpermissive face of Tus and the approaching helicase were challenged by biochemical and structural studies. These studies show that it is the helicase-induced strand separation that triggers the formation of new Tus–*Ter* interactions at the nonpermissive face – interactions that result in a highly stable "locked" complex. This controversy recently gained renewed attention as three single-molecule-based studies scrutinized this elusive Tus–*Ter* mechanism – leading to new findings and refinement of existing models, but also generating new questions. Here, we discuss and compare the findings of each of the single-molecule studies to find their common ground, pinpoint the crucial differences that remain, and push the understanding of this bipartite DNA–protein system further.

ARTICLE HISTORY
Received 26 June 2017
Revised 4 October 2017
Accepted 16 October 2017

KEYWORDS
DNA–protein interactions; DNA replication; prokaryotic replication; replication termination; replisome; Tus–Ter; single-molecule techniques; magnetic tweezers

Introduction

DNA replication in *E. coli* initiates at *oriC* and proceeds bidirectionally, creating two replication forks that invade the circular 4.6 Mbp chromosome in opposite directions. The forks progress at an average speed of about 1 kbp/s until they meet again at the terminus region roughly located opposite *oriC* (Figure 1(a)). As the replication forks approach the terminus, each encounters five 23 bp *Ter* DNA sites (denoted *Ter A–J*) bound in a specific orientation by a 36 kDa DNA-binding protein called Tus (Hill et al. 1987; Hidaka et al. 1989; Hill 1992; Kamada et al. 1996) and proceeds unhindered, implying dislodgement of Tus from *Ter* when the fork approaches from this "permissive" direction. However, when either fork continues beyond the first five *Ter* sites preceding the terminus region, Tus–*Ter* is approached from the opposite "nonpermissive" direction (Figure 1(a)), triggering it to bring the replication fork to a halt (Hill et al. 1987; Khatri et al. 1989; Hill and Marians 1990; Hill 1996). This arrangement therefore synchronizes the arrival of the two replication forks at the terminus by creating a trap for the first arriving fork, awaiting the late arriving one.

Each *Ter* site is nonpalindromic, does not contain any direct repeats and has a strictly conserved GC(6) base pair followed by a highly conserved 13 bp core region. Tus is a monomeric protein that forms a 1:1 complex with *Ter* (Figure 1(c)) (Coskun-Ari et al. 1994). The structure of the Tus–*TerA* complex shows that many of the

CONTACT Martin Depken s.m.depken@tudelft.nl Department of Bionanoscience, Kavli institute of Nanoscience, Delft University of Technology, van der Maasweg 9, 2629 HZ Delft, The Netherlands; Nicholas E. Dixon nickd@uow.edu.au Centre for Medical and Molecular Bioscience, University of Wollongong, New South Wales 2522, Australia; Samir M. Hamdan samir.hamdan@kaust.edu.sa Division of Biological and Environmental Science and Engineering, King Abdullah University of Science and Technology, Thuwal 23955-6900, Saudi Arabia; Nynke H. Dekker n.h.dekker@tudelft.nl Department of Bionanoscience, Kavli institute of Nanoscience, Delft University of Technology, van der Maasweg 9, 2629 HZ Delft, The Netherlands
*Present address: Department of Bioengineering, Stanford University, California, United States.
†Present address: Department of Molecular and Cell Biology, University of California Berkeley, California 94720, United States.

Supplemental data for this article can be accessed here.

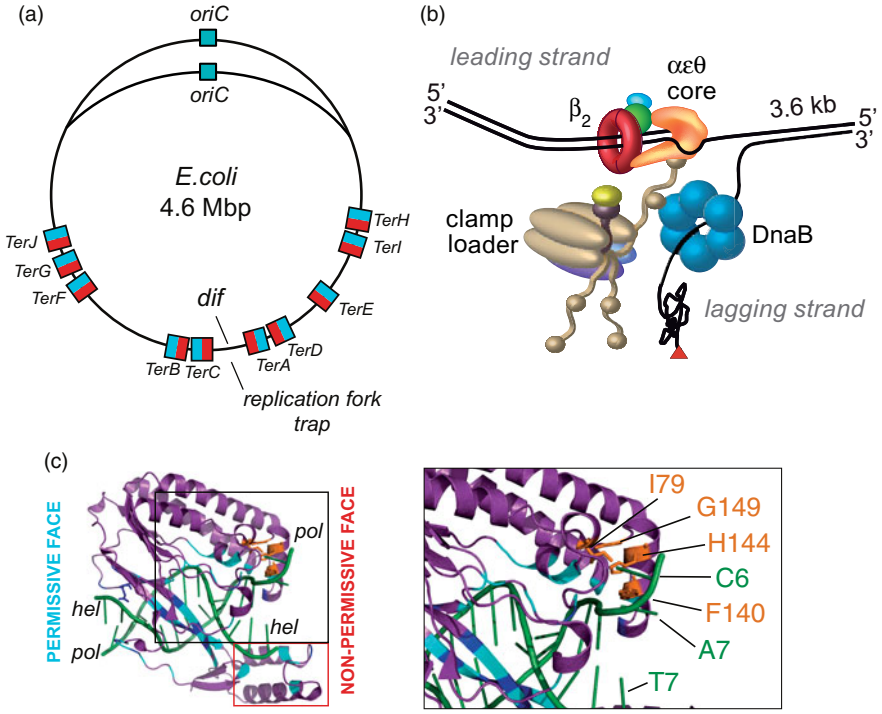

Figure 1. The Tus–*Ter* system. (a) DNA replication of the circular *E. coli* chromosome starts at *oriC* and proceeds bidirectionally. The two replisomes thus move in opposite directions and meet again around the *dif* site in the terminus region. Each replisome encounters five *Ter*-bound Tus proteins from the permissive side (cyan side), while *Ter* sites 6 through 10 are oriented nonpermissively (red side) for both replisomes. (b) Schematic representation of the *E. coli* replisome leading strand complex (Elshenawy et al. 2015). (c) The crystal structure of the Tus–*Ter* locked complex on forked *TerA* (green; the polymerase and helicase translocating strand are indicated as *pol* and *hel*, respectively) (Mulcair et al. 2006). Tus (purple) interacts specifically (blue) and nonspecifically (cyan) with the major groove of *Ter*. Residue R198 is in the α6/L3/α7 region (red rectangle). Upon strand separation at the nonpermissive face, the *Ter* C(6) base reorients itself to form specific interactions with several Tus residues in a 'lock pocket' (orange, see inset for details).

conserved residues among the *Ter* sites make base-specific contacts with the protein (Kamada et al. 1996; Neylon et al. 2005). The Tus–*TerB* complex has a reported dissociation constant (K_D) of 44 pM in 50 mM NaCl (Lee et al. 2014). This renders it the most stable complex known between a monomeric sequence-specific DNA-binding protein and a duplex DNA recognition sequence.

Tus–*Ter* is thought to have evolved specifically to block the *E. coli* replisome, a multi-protein complex that promotes DNA replication (Figure 1(b)). Many aspects of replisomal organization are conserved throughout all life forms from viruses to higher order eukaryotes (Benkovic et al. 2001; Johnson and O'Donnell 2005; Hamdan and Richardson 2009; Hamdan et al. 2009; van Oijen and Dixon 2015). At the front of the bacterial replisome is the hexameric ring-shaped DNA helicase, which encircles the lagging strand and moves in the 5′–3′ direction while unwinding DNA, thereby excluding and displacing the 3′–5′ leading strand template. DNA synthesis of the two daughter strands is carried out by DNA polymerases, enzymes that extend a primer in the 5′–3′ direction only, thus moving along a template strand in the 3′–5′ direction. The antiparallel nature of the double-stranded (ds) DNA helix necessitates simultaneous coordinated synthesis of two DNA strands with opposite polarity, leading to an asymmetric mechanism for nascent DNA strand synthesis: a continuous leading strand versus a discontinuous lagging strand DNA polymerization activity. *In vitro* assays can force the assembly of a leading-strand-only replisome by leaving out enzymes such as the primase required for repeated initiation of synthesis of lagging-strand DNA fragments.

The polarity of the DNA in the context of Tus–*Ter* is as pivotal to full understanding of this system, as it is to the DNA replication process itself. At each of the two faces of the complex, Tus interacts more extensively with one of the two double helical stands of *Ter*: at the non-permissive face this is the helicase-translocating lagging strand, whereas at the permissive face this is the polymerase-translocating leading strand (Kamada et al. 1996; Neylon et al. 2005). The C(6) base of *Ter*, which interacts with Tus to form the locked complex, is located on the leading strand template when Tus–*Ter* is

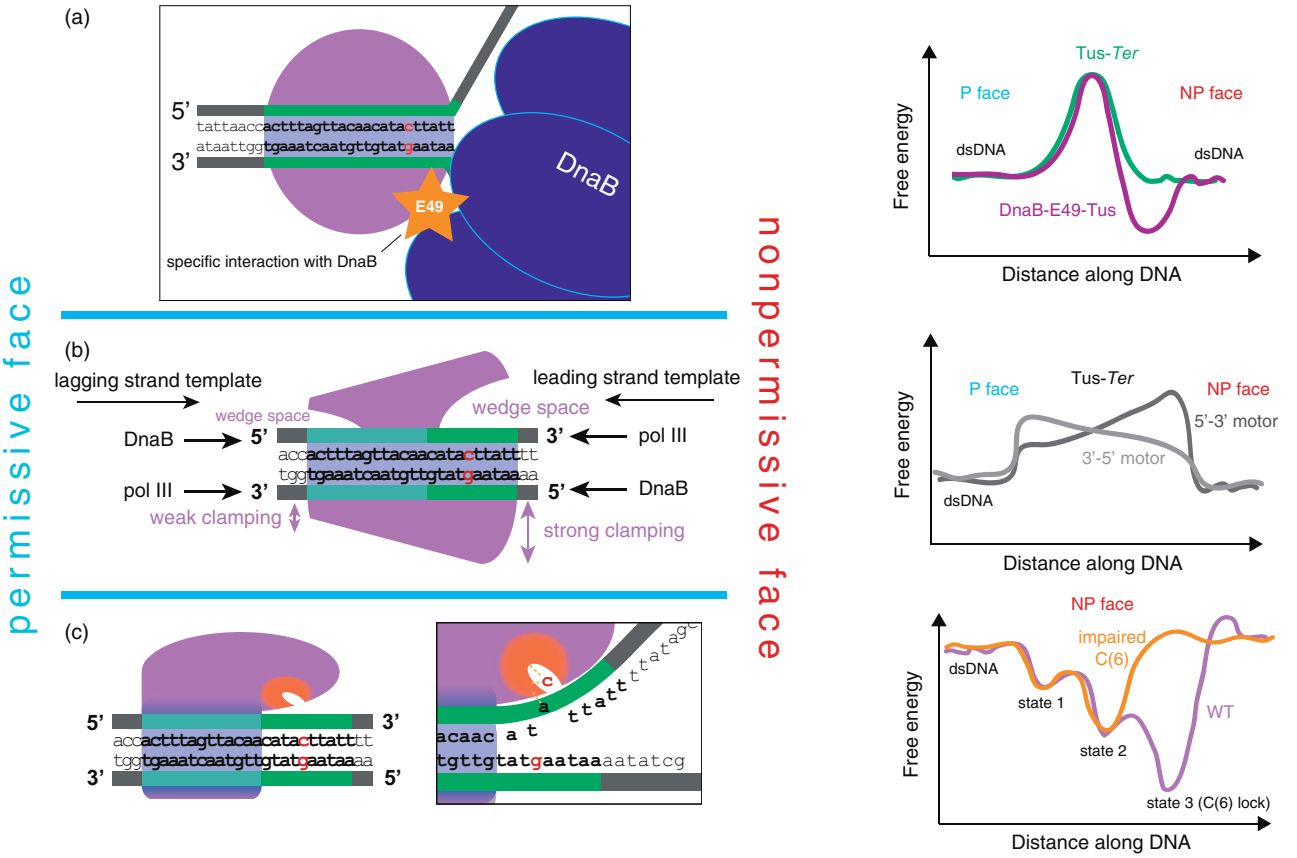

Figure 2. A schematic representation of the existing Tus–*Ter* models (left) and the corresponding energy landscapes (right). (a) The helicase interaction model: Left: the replicative helicase DnaB interacts specifically and physically with the non-permissive face of Tus–*Ter* (Mulugu et al. 2001; Bastia et al. 2008). Right: Tus–*Ter* forms a single, symmetric barrier along the DNA. A local energy minimum is formed only when specific helicase interaction (involving residue E49) at the nonpermissive face takes place, rendering the system capable of polar replisome arrest. (b) The dynamic clamping model. In this model, variations in the multitude and strength of binding interactions between Tus and along the *Ter* site lead to a different blocking efficiency at both faces (Kamada et al. 1996; Neylon et al. 2005) and thus explain polar arrest of various enzymes colliding with Tus–*Ter* (left: thickness of Tus (purple) is proportional to strength of interaction with *Ter*; right: stronger interaction between Tus and *Ter* implies a larger energetic penalty for an enzyme encountering these interactions). (c) The mousetrap model. Left: a specialized reorientation of the highly conserved C(6) base into a cytosine-binding pocket on the surface of Tus upon strand separation is what causes polar arrest (Mulcair et al. 2006). Right: Berghuis et al. (2015) showed that strand separation at the nonpermissive face allows for a three-step mechanism of binding of C(6) into its Tus-binding pocket, where each successive step draws the system further into an energetically favorable state.

approached at the non-permissive face, and on the lagging strand when approached at the permissive face of the protein–DNA complex (Figure 2) (Mulcair et al. 2006). Polar arrest by Tus–*Ter* must therefore involve a strand-specific mechanism sensitive to the polarity of translocation of the DNA motor.

Despite extensive studies over three decades, it has been surprisingly difficult to elucidate the role of Tus–*Ter* as well as the exact sequence of events that leads to asymmetric replication fork arrest at Tus–*Ter*. Besides this, it remains a mystery why Tus–*Ter* has evolved to be at most ~50% efficient *in vivo*, and why the chromosomal arrays of *Ter* sites are spread out over hundreds of kilobases (Figure 1(a)), all together covering almost half of the *E. coli* chromosome. Three mechanistic models have been proposed and debated: a helicase interaction model (Figure 2(a)) where the replicative helicase DnaB interacts specifically and physically with the nonpermissive face of Tus–*Ter* (Mulugu et al. 2001; Bastia et al. 2008); a dynamic clamping model (Figure 2(b)) where intrinsic differences in the strength of Tus–DNA interactions at the two faces of *Ter* lead to a different blocking efficiency (Hill and Marians 1990; Kamada et al. 1996); and a "mousetrap model" (Figure 2(c)), which suggests a specialized reorientation of the highly conserved C(6) base into a cytosine binding

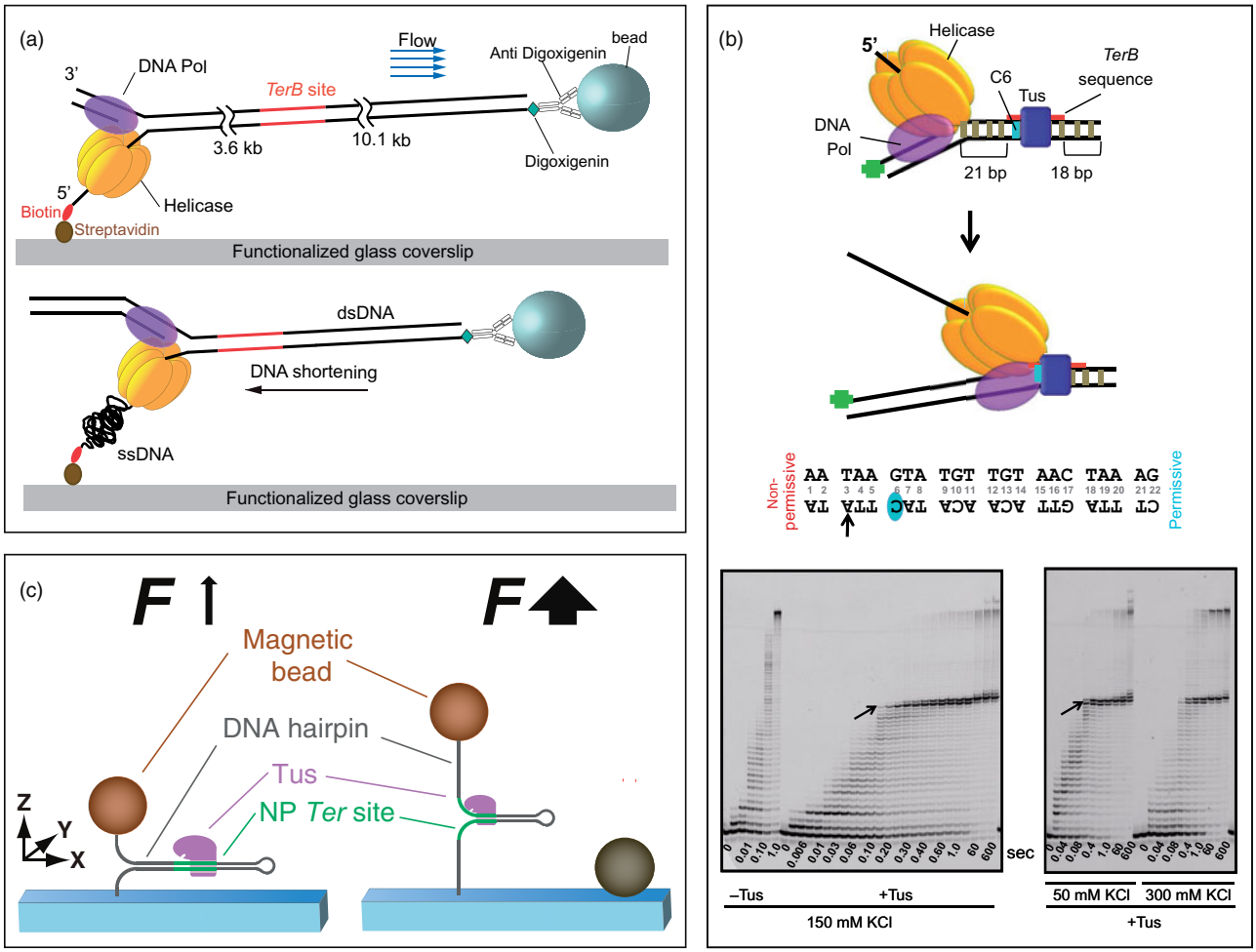

Figure 3. The three single-molecule assays discussed in this review. (a) The principles of the flow-stretching assay as used by Elshenawy et al. (2015) and Pandey et al. (2015). A forked double-stranded (ds) DNA template is anchored to a micron-sized bead and the surface of a flow-cell. The force exerted on the bead (~3 pN) by means of hydrodynamic flow is large enough to stretch the relatively rigid dsDNA, though too weak to have a similar effect on single-stranded (ss) DNA. A leading-strand synthesis complex progressively converts the surface-anchored lagging strand into ssDNA, thereby causing tether shortening that is inferred through the bead moving in the direction opposite to the flow (the replisome set up of Elshenawy et al. is shown in Figure 1(b)). (b) The quench flow assay as performed by Pandey et al. (2015), where the T7 replication machinery (helicase, polymerase or both) initiates synchronously on short ~60 bp forked dsDNA substrates containing a single *Ter* site. The reaction is stopped at discrete time intervals and products are gel-imaged. Arrows indicate the first arrest position band corresponding to the arrow on the *TerB* sequence shown above the gels. (c) The magnetic tweezers assay used by Berghuis et al. (2015), where a DNA hairpin containing a single *Ter* site (nonpermissive shown here) is positioned between a flow-cell surface and a magnetic bead. Lowering a pair of magnets towards the flow cell increases the upward pulling force on the bead. A force of 16 pN is sufficient to break the Watson-Crick base pairs and 'unzip' the dsDNA helix. This leads to a fully stretched ssDNA tether in the absence of Tus, or to the blocking of unzipping at Tus–*Ter* in the presence of Tus, in the latter case resulting in a shorter (by a characteristic length) ssDNA tether.

pocket on the surface of Tus upon strand separation causes polar arrest (Mulcair et al. 2006).

Here, we specifically discuss three recently published studies designed to further examine or integrate these models and unravel the mechanism of polar Tus–*Ter* replication fork arrest. A first study, by Pandey et al. (2015), examines the polar interaction of Tus–*Ter* when the heterologous bacteriophage T7 replisome, the isolated T7 replicative helicase, or the T7 DNA polymerase collide with this DNA roadblock. Two approaches are used here: a single-molecule flow stretching assay (Figure 3(a)), as well as a quench flow bulk-phase assay with single base pair resolution (Figure 3(b)). In a second study, Berghuis et al. (2015) investigate the sequence of events that lead to polar blocking of strand separation by probing the Tus–*Ter*

lock in an isolated fashion in a single-molecule magnetic tweezers assay (Figure 3(c)). Finally, in a third study, Elshenawy et al. (2015) reconstitute a leading strand *E. coli* replisome and observe single collision events with Tus–*Ter* in a single-molecule flow-stretching assay (as in Figure 3(d), but with the *E. coli* replisome as in Figure 1(b)). All studies probe either a wide variety of Tus mutants, altered *Ter* sites, or both, so as to discover the missing pieces of the Tus–*Ter* puzzle.

As we describe below, while the physical interaction model has recently become a less likely candidate, it is still unclear whether either of the other two is entirely correct. Both models have their merits, but most likely neither can stand alone in describing Tus–*Ter* fork arrest activity; instead, the recent studies suggest that Tus–*Ter* activity may be best described by a composite of the dynamic clamping and mousetrap models, of which more detailed mechanistic understandings await further discovery.

Overview of the three recent single-molecule studies

*Encounter of Tus–*Ter *complex by the heterologous bacteriophage T7 replisome*

Pandey et al. (2015) use a single-molecule flow-stretching assay (Figure 3(a)) as well as a quenched flow assay (Figure 3(b)) to examine the efficiency and details of Tus–*Ter* blocking the progression of the well-characterized heterologous bacteriophage T7 helicase and DNA polymerase. The use of a heterologous system is warranted because it is possible to synchronize initiation of DNA replication in the T7 system by preassembly of the replisome without Mg^{2+}, in contrast to *in vitro* replication by the *E. coli* replisome where loading of the DnaB helicase is inefficient in the absence of a natural origin of replication. Furthermore, it is possible to separately examine the effects of a Tus–*Ter* block on the separate activities of the helicase and polymerase as well as their coordinated activity. In the flow-stretching assay, helicase–polymerase–promoted bursts of DNA replication give rise to single-molecule trajectories of the number of synthesized base pairs over time as the helicase–polymerase approaches Tus–*Ter* from either direction. The quench flow assay allows for monitoring the last base incorporated before termination or pausing at Tus–*Ter* by the leading strand polymerase at single-base resolution, thereby providing details of the exact location of polymerase or helicase–polymerase stall sites. The quench flow assay also allows examination of helicase-independent T7 DNA polymerase strand-displacement activity and of polymerase-independent T7 helicase unwinding activity.

Nonpermissive Tus–*Ter* was shown to block the progression of the T7 helicase–polymerase as well as the T7 helicase. The leading-strand translocating DNA polymerase showed significant pausing at the nonpermissive face; however, full arrest of DNA polymerase strand-displacement activity only occurred at the permissive face of Tus–*Ter*. The blocking of the DNA polymerase at the permissive face – the face at which a C(6) interaction cannot be triggered through strand separation – strongly supports the notion of a Tus–*Ter* dynamic clamping mechanism. This reverse blocking effect also points toward a sensitivity of the Tus–*Ter* mechanism to the translocation polarity of the enzyme in question.

The quench flow data show that slowing of progression occurs upon interaction of the helicase–polymerase at nonpermissive Tus–*Ter*: within seconds, polymerase blockage at T(3) and (predominantly) A(4) of *Ter* are observed, while after a couple of minutes A(5) incorporation is also observed. These results demonstrate that DNA synthesis is permanently stopped before the GC(6) base pair, implying formation of the C(6) lock complex. *TerB* with altered C(6) was unable to permanently stop DNA synthesis, but pauses were still observed in both assays, with both the distribution of (minute-long) pause times in the flow stretching assay and the observation of sequential pause sites in the quenched flow assay being indicative of a multi-step fork arrest process independent of C(6) lock formation.

In summary, Pandey et al. (2015) show that Tus–*Ter* effectively blocks the progression of the T7 helicase–polymerase, indicating that the Tus–*Ter* blocking mechanism can occur independently of specific interaction with the *E. coli* DnaB helicase. The C(6) base is crucial to *permanent* stoppage of the T7 helicase–polymerase at the non-permissive face, yet the blocking of polymerase progression at the permissive face of Tus–*Ter* indicates that this DNA–protein system has also evolved to block entities with a specific translocation polarity. Prolonged pausing at *Ter* sites that do not form the C(6) lock is suggestive of an underlying multi-step process towards C(6) lock formation.

*Effect of strand separation on Tus–*Ter *complex in the absence of replication proteins*

Berghuis et al. (2015) examine the interaction strength of Tus–*Ter* upon strand separation by applying a force on single DNA hairpins containing a *Ter* site in either the permissive or nonpermissive

orientation (Figure 3(c)). DNA replication enzymes are not present to unwind duplex *Ter* DNA; rather, force-induced unzipping *mimics* the strand separation that normally accompanies DNA replication activity. Upon performing unzipping in the presence of Tus, the authors observe nearly unimpeded strand separation for *Ter*-bound Tus in the permissive orientation, yet blockage of strand separation is seen for *Ter*-bound Tus in the nonpermissive orientation, directly showing that components of the replisome are not required for the Tus–*Ter* C(6) lock to form. In fact, the lock forms much more efficiently than *in vivo* observations report (100% blocking of hairpin strand separation *vs.* ~50% reported *in vivo* and *in vitro* replication arrest efficiency), even though the rate of strand separation is ~20-fold higher than during replisome-mediated strand separation.

In these magnetic tweezers experiments, the strength of the Tus–*Ter* interaction is quantified by measuring the dwell time of the blocking of strand separation at a given force (typical $N \sim 100$). The distribution of these dwell times typically consists of three single-exponential distributions, which implies that three distinct states (characterized by their respective lifetimes) underlie the nonpermissive Tus–*Ter* interaction. The state lifetimes were shown to be the longest for the wild-type Tus–*Ter* interaction, while they decreased as mutations in the lock domain of Tus were introduced. The longest lived state is assigned to the C(6) lock formation. Mutations in the DNA-binding domain of Tus did not affect the state lifetimes, mutation of the *Ter* C(6) base disrupted lock formation more than any single mutation of Tus could induce, and specific mutation of Tus residue E49 (to K) led to a decrease in probability of the longest lived lock state. Preformation of the C(6) lock prior to strand separation did not alter either the probabilities or lifetimes of the three states, indicating that the Tus–*Ter* interactions have time to equilibrate during the process of force-induced strand separation.

Together, these results indicate that Tus–*Ter* lock formation at the non-permissive face is a three-step process. Tus-mutant E49K is shown to influence only the *probability* of the long-lived state – the chance of C(6) lock formation occurring – while leaving the strength of the C(6) interaction intact. For this reason, E49 is proposed to play a role in guiding C(6) to its final (full lock) position. The authors propose that the E49K experiments also show how enzymes could decrease the probability of full lock formation by sterically hindering the lock formation process through nonspecifically interacting with residues such as E49 upon collision. New data acquired for this Perspective shows that the lifetime and probability of the first two states can be altered by mutation R198A, while keeping the longest-lived state associated with C(6) lock formation intact (Figure 4(c)).

*Encounter of Tus–*Ter *complex by the* E. coli *replication fork*

Elshenawy et al. (2015) investigate how efficient Tus–*Ter* is at blocking the progression of DNA replication by the *E. coli* replisome by monitoring single replication events of a DNA template containing a *Ter* site in a single-molecule flow-stretching assay under conditions where the C(6)-lock is active or inactivated (Figures 1(b) and 3(a)). Data emerging from this assay consist of the number of synthesized base pairs over time. The *Ter* site is positioned 3.6 kb downstream of the site of replication initiation. When *Ter* is nonpermissively oriented, there is a significant increase in the occurrence of termination of DNA synthesis at this 3.6 kb position in the presence of Tus (~50%) compared to permissively oriented Tus–*Ter* (~11%), or termination at this site without Tus (~5%). Notably, these statistics reproduce those observed *in vivo*. Preforming the C(6) lock increases the efficiency of fork arrest to ~90%, suggesting that C(6) lock formation is an inefficient process in the presence of the replisome.

The single-molecule replication events are divided into groups based on whether DNA replication terminates (Stop), temporarily pauses (Restart), or proceeds unimpeded (Bypass) at Tus–*Ter*. By correlating these occurrences to the estimated replication fork velocities ($v \sim 500$–1500 bp/s), the authors find a positive correlation between the fork velocity and the probability of unimpeded bypass of Tus–*Ter* (Supplementary Figure S2). A similar positive correlation is observed when the lock is completely inactivated by replacing C(6) with G(6) or altering the C(6)-binding pocket (Tus-H144A). This suggests that the efficiency of Tus–*Ter* is determined by a step preceding C(6) lock formation. This step imposes transient stoppage only and is proposed to buy time to enable the inefficient C(6) lock formation. Mutation of the R198 residue that clasps the helicase-translocating lagging strand (to A) leads to a complete failure of Tus to permanently stop the fork; however, preformation of the lock fully undoes the detrimental effect of the R198A mutation. Triggering C(6) lock formation therefore requires R198 interactions to slow down the replication fork. Structural analysis suggests that melting the GC(6) base pair induces R198 to rearrange its interactions with TA(5) and G(6) from base specific to phosphate-mediated interactions. The authors therefore propose the existence of a head-to-

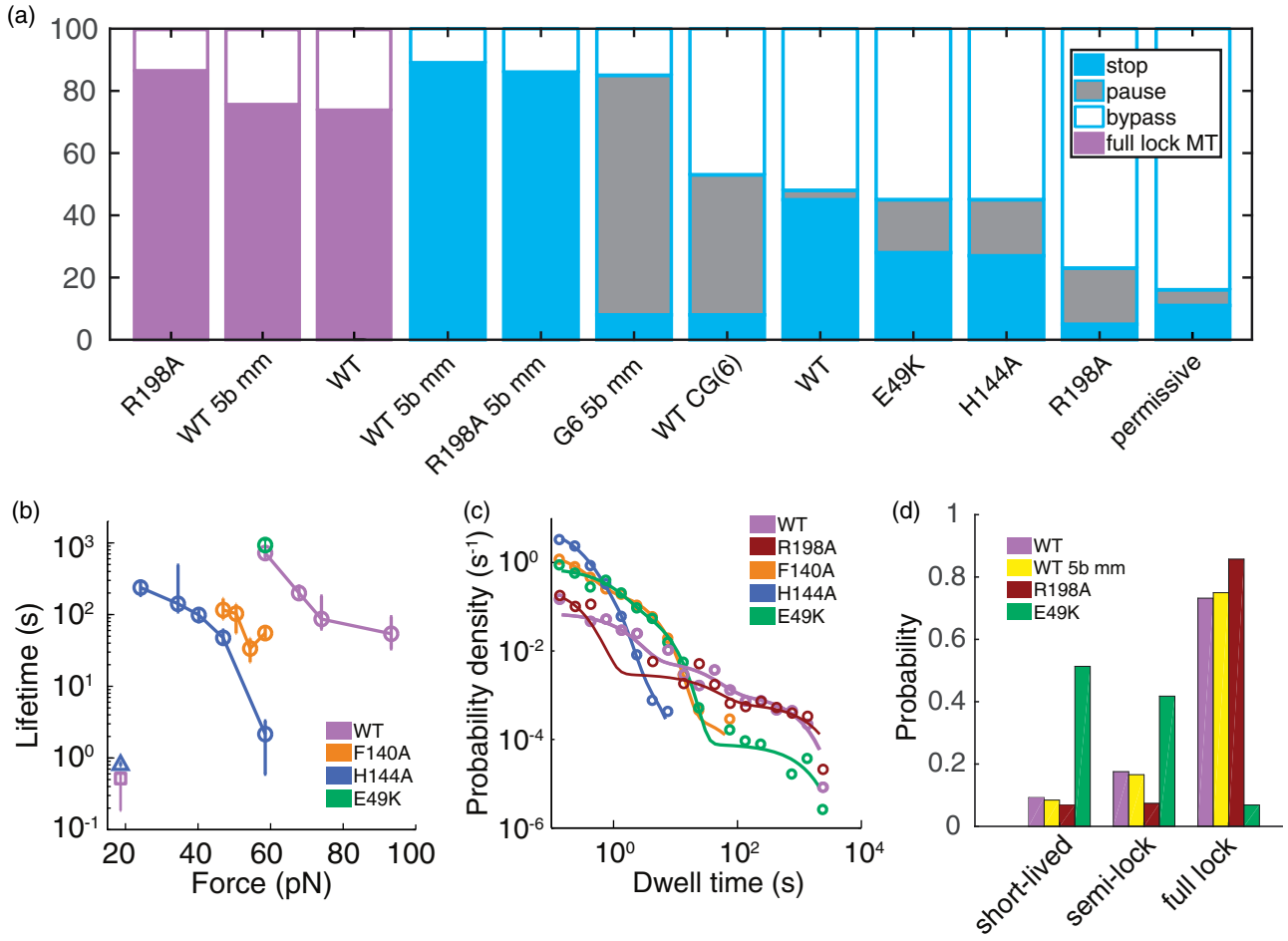

Figure 4. Quantifying Tus–*Ter* activity with a variety of assays. (a) The replisome stoppage (cyan), pause (gray) and bypass (white) probabilities, as measured by Elshenawy et al. (2015), as well as the full C(6) lock formation probability (purple) at an applied force of 59 pN as measured by Berghuis et al (2015). Wild-type Tus (WT) as well as site-specific Tus mutations (E49K, H144A, R198A) and/or *Ter* mutations ('CG(6)' = inversion of GC(6); "5 b mm" = the 5-base mutation-induced mismatch required to pre-form the lock) are shown. "Permissive" denotes the singular case where strand-separation is induced at the permissive face. (b) The fit lifetimes of the longest-lived exponential of nonpermissive (circles, colored as indicated) for Tus-WT, E49K, F140A and H144A over the measurable range of forces extracted with the MT assay. The combination of H144A with an inversion of GC(6) to GC(6) (blue triangle) reduces the force-dependent lifetime of this specimen to permissive WT Tus–*Ter* barrier-like (purple square) proportions. (c) The full distribution of MT-induced lifetimes at 59 pN (circles) as well as the 2 or 3-exponential fit (solid line). (d) The MT state probabilities at 59 pN for the Tus–*Ter* species showing C(6) full-lock interaction: WT (purple), R198A (red-brown), WT Tus combined with a DNA hairpin containing a *Ter* site with mismatched bases 3–7 (5 b mm) at the nonpermissive end (the only known procedure to pre-form C(6) interactions artificially, yellow), and E49K (green). "Short-lived", "semilock" and "full lock" denote the states associated with the three single exponentials found for these species, where the longest-lived exponential corresponds to C(6) lock formation (full lock). (e) The ds*Ter*:forked-*Ter* ratio of the dissociation constants (K_D) of various Tus species (SJ, unpublished data). A ratio larger than 1 (dashed horizontal line) depicts strengthening of the complex upon making C(6) freely available, a strong indicator of C(6) lock formation. (f) The force-dependent trend in full C(6) lock formation probability (purple circles, error bar is 1-σ confidence interval obtained through bootstrapping), as extracted through fitting the 3-exponential lifetime distributions of WT Tus–*Ter* over a range of forces. Fitting of the sigmoid function (solid lines; fits to data (purple) as well as upper (orange) and lower (cyan) confidence bounds are shown) associated with Kramer's theory for reaction kinetics (see main text for details) to these data provides an estimate for the force at which this force-induced full-lock probability equals the stoppage probability (horizontal dashed line) of the replisome encountering WT Tus with a preformed lock (the cyan "WT 5 b mm" shown in (a)). This provides a first estimate of the force required to stall the *E. coli* replisome (~56 pN, 51–62 pN 1-σ confidence interval range, see inset for details).

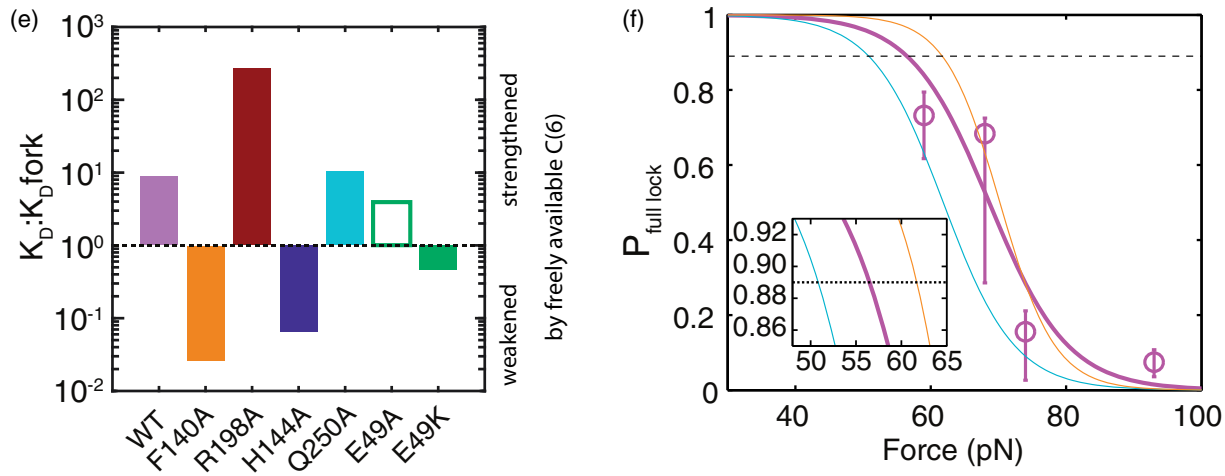

Figure 4. Continued.

head kinetic competition between the rate of strand separation by the replisome and the rate of rearrangement of R198 interactions.

Taken together, these flow-stretching experiments suggest that the efficiency of replication termination depends on the velocity of the replication fork that collides with Tus–*Ter*. The observations also suggest that while the C(6) interaction forms a crucial part of the Tus–*Ter* interaction upon strand separation at the nonpermissive face, it is a preceding step in which R198 interacts with the strand complementary to C(6) that is critical in stopping the replisome in that it buys time for triggering inefficient C(6) lock formation.

Discussion

Assessing the relative roles of helicase interactions, dynamic clamping, and the C(6) lock in establishing polar fork arrest

The studies of Pandey et al. and Berghuis et al. suggest that, of the three proposed Tus–*Ter* models, the helicase interaction model does not constitute the dominant mechanism for polar Tus–*Ter* arrest. Pandey et al. show that the heterologous T7 replication machinery is blocked efficiently at non-permissive Tus–*Ter*. This observation cannot report on any physical interactions that might occur between the *E. coli* DnaB helicase and Tus; however, these authors have also specifically sought to detect physical interaction between Tus and DNA-bound DnaB in a variety of formats by surface plasmon resonance, yet to date no manifestation thereof has been found. Moreover, by performing their mechanical strand separation experiments in the absence of any replicative enzymes whatsoever, Berghuis et al. directly show that helicase interactions are not required for Tus–*Ter* to effectively block DNA strand separation at its non-permissive face.

The T7 quench flow study postulates a dynamic clamping mechanism to account for the observed specificity in blocking the T7 helicase at the nonpermissive face. The blocking of polymerase activity at the permissive face is explained by specific interactions between Tus and the leading strand template (i.e. the 3′–5′ directed strand, Figure 2(b)). This observation implies that there are inherently different types of DNA–Tus interactions at the respective faces of Tus–*Ter*, consistent with the crystal structure of Tus bound to a fully ds*Ter* site (Kamada et al. 1996) and reflective of dynamic clamping. More specifically, these observations suggest Tus–*Ter* has evolved to block a strand separation process that allows the 3′–5′-oriented strand more degrees of freedom to interact with Tus than the complementary strand. In other words, Tus–*Ter* seems to have evolved to block the process of strand separation at the nonpermissive face induced by an enzyme moving along the 5′–3′ lagging strand template. The canonical process through which this occurs is of course *E. coli* DNA replication mediated by a replisome spearheaded by the DnaB helicase.

However, the force-induced DNA hairpin unzipping experiments, which directly show that Tus–*Ter* blocks strand separation at the nonpermissive but not the permissive face, are difficult to explain through dynamic clamping alone. Not only would the enormous difference in observed blocking be hard to explain through this mechanism, but furthermore, in contrast to predictions of the dynamic clamping model, Berghuis et al. also directly show how Tus amino acid residues showing no interaction with *Ter* DNA in the ds*Ter* crystal structure (Kamada et al. 1996) have a dramatic effect on

the polar blocking of strand separation when altered (Figure 4(c,d); E49K).

In fact, all three studies reviewed here suggest at least some evidence for a specific interaction of C(6) with its lock pocket, a key ingredient of the mousetrap model. For instance, the quench flow assay showed the formation of a variety of products representing polymerase stalling sites from T(3) through A(5), with the majority being at A(4), while incorporation of G(6) was never observed. Both Pandey et al. and Elshenawy et al. show that inverting the GC(6) base pair has dramatic consequences for the incidences of (permanent) arrest in the single-molecule flow stretching assays, and improvements in arrest efficiency are observed when the C(6) lock is allowed to form before any interactions with the replication fork occur (Figure 4(a)). Previous work by the group of Bastia showing that an isolated DnaB helicase translocating on dsDNA was blocked at the nonpermissive face of Tus–*Ter* can be interpreted as evidence against involvement of C(6) lock formation (Bastia et al. 2008). The authors further supported this argument by showing fork stoppage still occurred when base pairs 4 and 5 of *Ter* are in covalent interstrand crosslinks to prevent any strand separation from occurring before C(6). However, these results may be reinterpreted in light of the new evidence presented by Elshenawy et al. showing the rate-dependent fork arrest activity and the ability of Tus–*Ter* to permanently stop the replication forks in a C(6) lock-independent mechanism, as discussed below. These results suggest that the more slowly moving DnaB used in the earlier experiments (Bastia et al. 2008). could be efficiently blocked without requiring C(6) lock formation.

There is more to locked complex formation than C(6) interactions alone

All three studies show there is more to Tus–*Ter* activity than C(6) interactions alone. This is exemplified by impairing C(6) lock formation either through mutating the Tus residues shown to interact with C(6) in the locked state or altering the *Ter* C(6) base itself. In either instance, interactions become weaker (MT study, Figure 4(b–d)) or a large fraction of the halts turn from being permanent to transient (enzymatic assays, Figure 4(a)). However, it is clear that a significant barrier remains, much more so than the barrier imposed by permissively oriented Tus–*Ter* (Figure 4(a,b)).

More specifically, when comparing the outcome of a CG(6) inversion in the flow-stretching experiments (Figure 4(a), "WT CG(6)", cyan) with that of the wild-type lock (Figure 4(a), "WT", cyan), the occurrence of bypass events is indistinguishable. The absence of C(6) interaction that is a result of this inversion turns a large fraction of permanent stoppage into transient stoppage. Permanent stoppage turned transient implies a lowering of the Tus–*Ter* induced barrier, while at the same time the bypass frequency remains unaffected. Taken together, these specific replisome experiments point towards the existence of a barrier independent of C(6) interactions.

The application of force in the MT assay readily allows for a separation of a variety of Tus–*Ter* strand separation-induced energy barriers, as exemplified by the reproducible occurrence of the multiexponential distributions (Figure 4(c)). In addition, in the MT experiments, the severely reduced barrier imposed by the lock-defective mutant H144A reduces to permissive Tus–*Ter* proportions when H144A is combined with a CG(6) inversion (Figure 4(b)): this provides a strong indication that both C(6) and G(6) interactions play a role in barrier formation. We also find in the flow-stretching assay that there is still significant permanent (28%) replisome stoppage imposed by Tus-E49K (M.M.E. and S.M.H., unpublished data; Figure 4(a)); E49K shows very similar amount of stoppage as Tus-H144A), while it is highly unlikely that C(6) interactions form with E49 in the event of enzymatic unwinding (Mulcair et al. 2006). Thus, both the studies of Berghuis et al. and the studies of Elshenawy et al. find that a significant barrier is imposed by Tus–*Ter* in a situation where C(6) does not locate its lock pocket, as witnessed by the continued presence of the first two states in the MT experiments with E49K, F140A and H144A (Figure 4(c)) and by the continued occurrence of permanent stoppage with E49K and H144A in the functional assays (Figure 4(a)).

Other key actors in polar arrest: R198

Besides the amino acid residues that directly interact with C(6) in the lock pocket, there are several other key players that are known or at least suspected, to play a pivotal role in forming the Tus–*Ter* lock. R198 and E49 are two such residues. From the crystal structures of Tus bound to ds*Ter* and in the lock state on forked *Ter*, it is apparent that structural rearrangements take place in the R198 region that interacts with the lagging strand template upon lock formation. Specifically, R198 interacts with the A(5) and G(6) bases of this strand, with Elshenawy et al. suggesting additional interactions with T(5) on the leading strand, consistent with Mulcair et al. (2006). In the locked complex, these R198–A(5)/G(6) interactions have made place for interactions of R198 with the phosphate backbone of the lagging strand, between bases 6 and 7. Observing severely impaired replisome blocking for Tus mutant R198A in flow

stretching experiments, Elshenawy et al. suggest that R198 transiently holds the two strands together by interacting with base pair 5 of *Ter*, rendering it a rate-limiting step in the process toward C(6) lock formation. They also show that, similarly to the impaired CG(6) lock, the R198A-blocking behavior is restored to wild-type proportions when the lock is allowed to preform (Figure 4(a), bypass of "R198A 5 b mm" equals "wt 5 b mm" (in cyan)). When R198A is subjected to hairpin pulling experiments, Berghuis et al. (unpublished) observe full C(6) lock formation (Figure 4(a), "R198A" in purple) similar to that observed for wild-type Tus–*Ter*, but now showing a marked difference in the lifetime or probability of the first and second lock states, respectively (Figure 4(c,d), in brown), suggesting that either one of these states reflects the magnitude of R198–*Ter* interactions. Taking both observations into account, it indeed appears that rearrangements involving R198 form a step towards C(6) lock formation, while concomitantly linking the measurements observed in MT and the enzymatic single-molecule assays.

Other key actors in polar arrest: E49

Tus-E49K has been reported to be deficient in polar arrest of replication forks *in vivo* (Sahoo et al. 1995; Mulugu et al. 2001), and a specific interaction between DnaB and this Tus residue has been hypothesized (Bastia et al. 2008). A more subtle and refined role for E49 was proposed by Berghuis et al. based on the observation that hairpin unzipping experiments on E49K–*Ter* revealed that full wild-type-like lock formation could still occur, but with a dramatically decreased probability ($P_{\text{full lock}}(\text{WT}) = 79\%$; $P_{\text{full lock}}(\text{E49K}) = 7\%$ at 59 pN). The other two lock states were identical to the corresponding states found for F140A (Figure 4(c); F140A has no full-lock signature as C(6) interactions do not occur). This suggests a possible mechanistic role for residues outside the Tus lock pocket, in which they help to guide C(6) toward its final, fully locked position. This proposition is consistent with the crystal structure of the lock complex, which shows a water-mediated H-bond between E49 and the 5′-phosphate of A(7) (Mulcair et al. 2006). Berghuis et al. hypothesize that the decrease in probability observed *in vivo* compared to the MT lock probability could find its origin in this C(6)-guiding mechanism, as the physical presence of an enzyme at the nonpermissive face of Tus–*Ter* could perturb the guiding process, rendering it less efficient. In essence, Berghuis et al. suggest that the presence of replicative enzymes at the non-permissive face of Tus–*Ter* influences the reaction equilibrium of lock formation.

The E49K-induced effects in both MT and functional assays couple the decrease in likelihood of lock formation directly observed in the hairpin experiments to an additional decrease in blocking probability caused by the presence of an enzyme moiety at the fork. In other words, blocking of the *E. coli* replisome by Tus-E49K will become even less likely than the blocking of strand separation in the presence of E49K in the hairpin pulling experiments. A prediction would be that preformation of the lock (e.g. "E49K 5 b mm") in replication assays would restore the probability of observing a blocking event to a similar order of magnitude observed for E49K in the hairpin experiments. In the hairpin experiments, lock preformation using E49K led to similar behavior to E49K on a wild-type *Ter* site (i.e. E49K 5 b mm behaved like E49K; Berghuis et al. 2015), just like preforming the lock did not induce a change with WT Tus–*Ter*.

The presence of enzymes at the fork changes the game

The pre-existence of strand separation in the functional assays, induced through a 5-base mismatch ("5 b mm") at the nonpermissive face of *Ter*, significantly reduces the bypass probability. This is irrespective of whether the C(6) lock is activated, as inactivation of C(6) interaction by mutation to G(6) results in permanent interactions becoming transient (i.e. without changing the probability of bypass, as discussed earlier). This drop in bypass probability upon preexistence of strand separation suggests that presence of helicase and/or polymerase influences the effect of the C(6)-independent barrier.

The MT experiments, where there is never an enzymatic presence at the fork, confirms the "enzyme effect" by showing identical results for hairpin pulling experiments with a preformed lock and those with a wild-type *Ter* site (Figure 4(d)). This is contrary to the experiments carried out with enzyme-induced fork propagation, where alterations of the *Ter* site allow the lock to preform but will thus always need to be performed with a non-native *Ter* site to ensure a region of unpaired bases around C(6). Taken together, these findings suggest that a nonphysical helicase–Tus interaction might occur after all, yet with the opposite effect of decreasing rather than promoting the efficiency of polar arrest.

Extension of the mousetrap model: a composite mechanism underlying polar arrest

In light of the studies discussed here, it is now possible to dovetail parts of the models proposed. A common feature of the three single-molecule studies is that

Tus–*Ter* blocking is a multistep process. Both Berghuis et al. and Elshenawy et al. propose an extended version of the mousetrap model, where C(6) interaction with the Tus lock pocket is the (third and) final step toward a locked state. Both works hypothesize that the series of events leading to this C(6) lock state are most likely to be sequential. Presumably a result of the intrinsically different nature of the two assays, both studies propose slightly different versions of a locking mechanism, making assumptions their own data support. Berghuis et al. show that the C(6) state is the strongest interaction and propose a three-state kinetic model where interaction progressively strengthens on progression from one state to the next. Elshenawy et al. emphasize and propose that R198 rearrangement is rate limiting, so as to allow time for C(6) to find its pocket, as they observe a clear correlation between the single-population replisome velocity and the probability of fork stalling at nonpermissive Tus–*Ter* (see Supplementary Discussion and Figure S2 for further details).

The Elshenawy et al. and Pandey et al. works provide evidence that a composite mechanism of dynamic clamping and C(6) mousetrap best describe Tus–*Ter* fork arrest activity at the nonpermissive face. Both studies favor the existence of a composite mechanism based on the assumption that C(6) lock formation is an inefficient process. In support of this inefficiency, 10% and 50% run-off DNA synthesis beyond the nonpermissive face of Tus–*Ter* are reported for the slow T7 and fast *E. coli* replication forks, respectively. Preforming the C(6)-lock in both cases severely reduces the run-off DNA synthesis, supporting the observation that the run-off is caused by inability to trigger the C(6)-lock.

Elshenawy et al. suggest that the operation and relevance of this composite mechanism are determined by how far the helicase unwinds the *Ter* site before Tus is able to stop it. Maintaining the clasping on the DnaB-translocating lagging strand by its interaction with R198 is critical to prevent DnaB from advancing farther into Tus–*Ter* central interactions. Mutating R198 to A results in complete failure of Tus–*Ter* to permanently stop the replication fork (Figure 4(a)), although Tus-R198A remains able to form the C(6) lock complex. Indeed, a preformed C(6) lock with Tus-R198A is able to fully stop the replication fork (Figure 4(a)), demonstrating that clasping the DNA by R198 interaction is a prerequisite to enzyme-induced triggering of the C(6) lock complex. This path of dynamic clamping by R198 interactions that is followed by triggering the C(6) lock is compulsory when the helicase melts *Ter* beyond the GC(6) base pair. Mimicking this scenario by preforming a Tus complex with a mismatched bubble in place of base pairs 3–7 with the C(6) locking mechanism also being inactivated by altering C(6) (G(6) 5 b mm) fails to impose permanent fork stoppage, while the same substrate with an activated C(6) locking mechanism (WT 5 b mm) imposed highly efficient permanent fork stoppage (Figure 4(a)). Elshenawy et al. further show that R198 interactions are able to impose permanent fork stoppage if the replisome does not melt *Ter* beyond the GC(6) base pair. This is shown by the ability of the lock-defective mutant Tus-H144A to impose significant permanent fork stoppage that is half of that observed by wild-type Tus (Figure 4(a)); the other half that are still stalled transiently would represent events that require stoppage by the C(6) locking mechanism after being transiently halted by R198 interactions. These results confirm previous findings of the operation of a C(6) lock-independent mechanism leading to permanent fork stoppage (Mulugu et al. 2001; Bastia et al. 2008) and pin it down to the interactions of R198.

A structural comparison of the C(6) locked complex with Tus bound to the wild-type ds*Ter* site or an altered ds*Ter* site with reversed GC(6) suggests that melting the GC(6) base pair provokes R198 to rearrange its interactions with TA(5) and G(6) from base specific to phosphate-mediated interactions. The authors therefore propose that a fast-moving replisome melts *Ter* site beyond GC(6) and outcompetes the rate of rearrangement of R198 interactions, whereas a slower replisome will be effectively stopped by either the C(6) lock-independent mechanism (if R198 interactions are unperturbed) or by the C(6) lock-dependent mechanism (if R198 interactions are perturbed and R198 rearranges its interactions with the lagging strand).

Further synergistic insights: alignment of magnetic tweezers data with binding studies

A point of interest is a subtle divergence between the results of hairpin pulling experiments (Berghuis et al. 2015) on the one hand and binding studies and crystallography on the other for Tus mutants that include E49K (S.J. and Zhi-Qiang Xu, unpublished). Using surface-plasmon resonance (SPR), the effect of C(6) lock formation can be observed on a forked *Ter* substrate and compared to the kinetics of binding on a wild-type ds*Ter* site (Figure 4(e)). Such experiments reveal an order of magnitude decrease in K_D upon C(6) lock formation for WT Tus–*Ter*, whereas Tus species with mutations in residues that directly interact with C(6) (F140A and H144A) instead display an increase in K_D, suggesting an absence of C(6) interactions. By this standard, Tus mutants that maintain C(6) interactions include Q250A, R198A and E49A, whereas those that do not include F140A, H144A and E49K (Figure 4(e)). In

contrast, the hairpin pulling experiments do report C(6) interactions for E49K, yet with a dramatically decreased probability. The fact that the MT experiments observe (a small population of) C(6) lock formation could imply a pulling bias (see Supplementary Discussion and Figure S1 for further details). However, when observing the aforementioned K_D-associated C(6) lock formation signature in the less invasive mutation E49A (with a binding profile signature most closely related to wt Tus), we consider that this residue plays its suggested C(6) guiding role.

Further synergistic insights: a first estimate of the E. coli *replisome stalling force*

In addition, it might now be possible to quantify the stall force of an *E. coli* leading strand replisome for the first time. The probability for full C(6) locking behavior of wild-type Tus–*Ter* is obtained by fitting the kinetic three-state model to the hairpin pulling datasets, which turned out to be 79% at 59 pN, reducing to 8% at 93 pN. As experiments have shown that the situation obtained in the hairpin pulling experiments is the same as (and should be compared directly with) the probability of blocking observed when the Tus–*Ter* lock is allowed to pre-form, the 89% blocking behavior of the *E. coli* replisome with a preformed lock (Figure 4(a)) suggests that the stall force is lower than 59 pN (which shows 79% lock formation). Assuming that full-lock formation is the result of a competition of rates between a fully locked and an unlocked state allows us to apply Kramer's theory of reaction kinetics and fit the expression $P_{\mathrm{lock}} = 1/(1 + \exp[-(F_{\mathrm{eq}}-F)\Delta x/k_{\mathrm{B}}T])$ to the trend in the force-dependence of the full lock state (Figure 4(f)). Here, F_{eq} is the force at which $P_{\mathrm{lock}} = 0.5$, F is the applied force, Δx the distance between the locked and the unlocked state, k_{B} is the Boltzmann constant and T the absolute temperature (see Supplementary Discussion for details). The force at which $P_{\mathrm{lock}} = 89\%$ shows that the upper boundary of replisome stall force is ~56 pN (Figure 4(f)). The effective distance to the transition state is ~0.7 nm.

*A coherent view on Tus–*Ter *efficiency*

We can now bring the findings of the previous subsections together to arrive at an overall model that describes how a replisome is stopped at Tus–*Ter* (Figure 5). The findings of Berghuis et al. and Elshenawy et al. taken together indicate that the probability of being stopped at Tus–*Ter* most likely finds its origin in that certain barrier formation rates are altered by the presence of the replisome. As the combined studies have made plausible, a likely candidate residue involved in rate-dependent barrier formation is Tus residue R198. R198 is in the α6/L3/α7 region that is located at the forefront of the non-permissive face of Tus (red rectangle in Figure 1(c)), making interactions primarily with the lagging strand and therefore likely to encounter the helicase first. It is possible that during rearrangement of R198 interactions that Tus might experience larger conformational changes in the α6/L3/α7 region that might also include transient dislodgment of R198 from the DNA. Such a scenario would shift the kinetics of rearrangement of R198 interactions to a much slower range. The findings of Elshenawy et al. suggest that presetting the path for C(6) lock formation via R198 interactions is necessary for C(6) to find its pocket. When subjected to the hairpin pulling experiments, Berghuis et al. show that Tus-R198A produces a C(6) full lock signature almost identical to wt Tus–*Ter*, indicating that C(6) interactions still occur (Figure 4(c,d)). However, a marked decrease in the occurrence of the intermediate lifetime barrier (Figure 4(c)) also occurs, and the lifetime of the first, short-lived state decreases (Figure 4(d)). This directly links R198 interactions to two of three rate-limiting steps found for Tus–*Ter* nonpermissive interactions. It is likely therefore that the replisome significantly deviates the path to C(6) lock formation not only by influencing side chain interactions such as with E49 as proposed by Berghuis et al., but also by trapping larger conformational changes in Tus that are incompatible with C(6) lock formation.

Conclusions and future directions

The work presented here and in recent articles defines a new and clear step towards unraveling the mechanism behind asymmetric blocking of replication forks by Tus–*Ter*. Linking the observations of hairpin pulling experiments and replisome flow stretching experiments leads to a mutual improvement of experimental interpretation. In this Perspective, we have for instance demonstrated that the conclusions involving R198A of Elshenawy et al. facilitate the interpretation of the change in the distribution of dwell times that R198A hairpin pulling experiments invoke. The hairpin pulling experiments offer a unique insight into the dynamics of isolated lock formation, without the need of lock preformation and its attendant alteration of *Ter*. Using the trend in wild-type "full locking" probability and comparing it with the stall probability of a replisome upon collision with a pre-formed Tus–*Ter* lock, we can now (roughly) quantify the stall force of a replisome for the first time (~56 pN). The discussed works also reveal the power of single-molecule studies, for the kinetic details

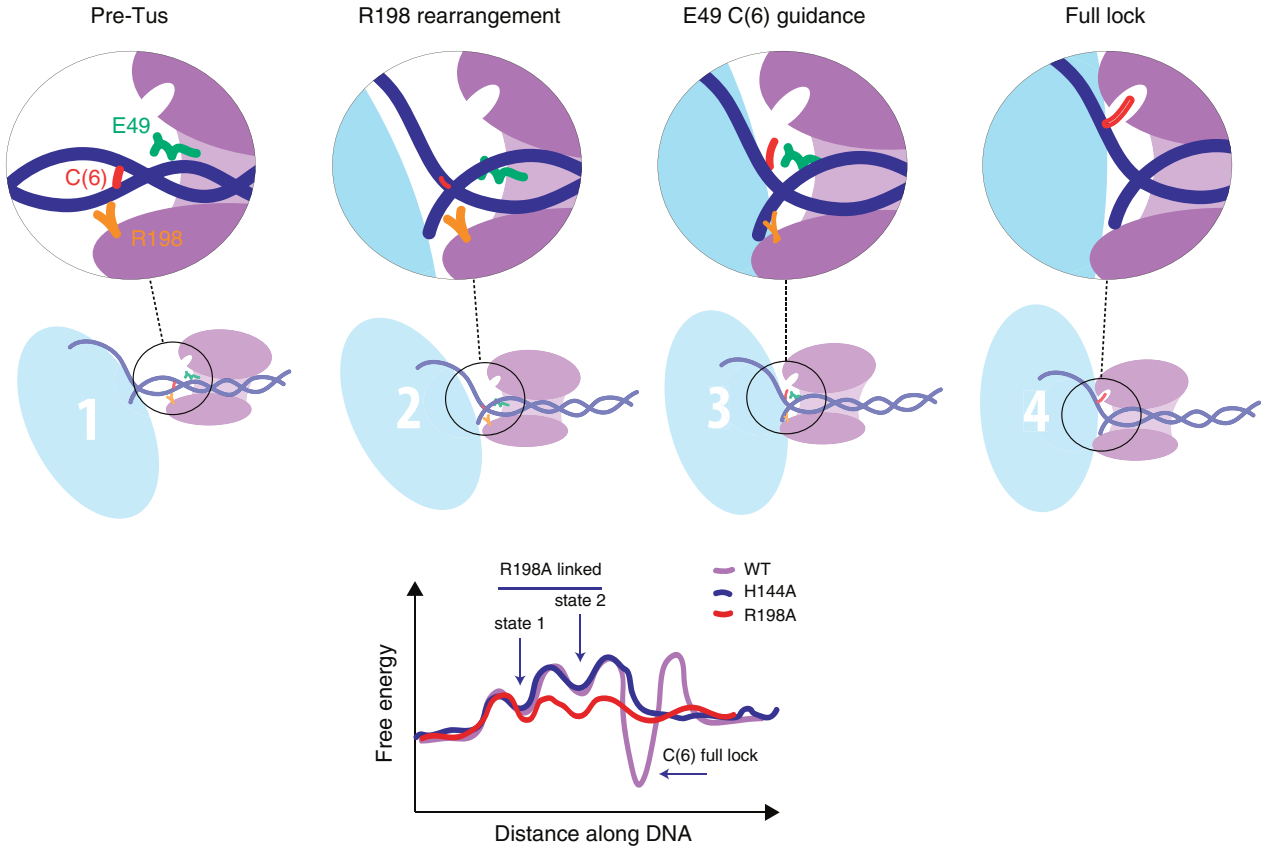

Figure 5. Schematics and energetics of the composite Tus–*Ter* model. Four-step schematic of the DnaB helicase (light blue) encountering *Ter*-bound Tus (purple): (1) pre-Tus; (2) R198 rearrangement; (3) E49-guided C(6) flipping in the presence of enzyme; (4) full-lock formation. DNA (blue), C6 (red), R198 (orange), E49 (green). Tus undergoes slight conformational rearrangements as lock formation progresses. Illustrative energy landscape diagram: Tus–*Ter* interactions that need to be broken or rearranged come with an energetic penalty (hence form a barrier). C(6), once in the Tus pocket, forms a local (thus stable) minimum in the landscape. Yet the absence of specific Tus residues or steric hindrance, changes the landscape and prevents the local minimum being reached, as our studies show. All energy landscapes are envisioned in the presence of DnaB; for example, Tus-R198A (red) follows a different trajectory in the absence of DnaB (MT with lock preformation).

of the dynamic, strand-separation-dependent biochemical events at the non-permissive face of Tus–*Ter* would not have revealed themselves using classical ensemble measuring techniques. The inherently different nature of protein–DNA interactions at opposing faces of Tus–*Ter* (i.e. dynamic clamping) mainly points toward evolution of Tus–*Ter* to specifically block entities moving along the 5′–3′ directed strand. However, it is evident that blocking of Tus–*Ter* at the non-permissive face cannot occur without structural rearrangements taking place – rearrangements culminating in insertion of C(6) into the Tus lock pocket. What was first coined the mousetrap model remains the most convincing model for Tus–*Ter* action to date, yet the recent single-molecule studies have led to its expansion into an extended (multistep) mousetrap model. We now know that the mousetrap, once triggered, is not a single hinge that flips and blocks fork progression once and for all, but a multi-state process with delicate reaction equilibria, equilibria easily perturbed by enzyme-induced steric interactions. Rearrangement of DNA–protein interactions at the lagging strand involving R198 is one of these steps, and there is likely an additional rearrangement that awaits discovery, as Berghuis et al. find three rate-limiting processes that give rise to Tus–*Ter* lock formation. Single-molecule assays will quite likely be the best way to go forward here.

There remain a number of open questions to address: (i) A subsequent step towards more intricate linking of the single-molecule experiments would, for example, be to follow *E. coli* replication fork progression as it collides with a pre-formed E49K Tus–*Ter* site, or to examine the barrier G(6) imposes on the lagging strand through subjecting a mismatched *Ter* GG(6) to the hairpin assay. Furthermore, (ii) it would be of interest to expand the selection of molecular motors beyond *E. coli* and bacteriophage T7 that support the Tus–*Ter* rate-dependent fork arrest activity while focusing on the rate, power stroke and geometry of strand pulling in

these motors. (iii) Further investigation of possible variation in replisome conformation and potential conformational changes in Tus during strand separation would require different kinds of assays than those discussed here. Single-molecule FRET would offer additional insights, as there might be a correlation between replisome stall probability and Tus–Pol III distance or conformational changes in Tus. (iv) The proportion of replication forks stalled at Tus–*Ter* has been consistently reported to be ~50% *in vivo* (Valjavec-Gratian et al. 2005; Duggin and Bell 2009), and Elshenawy et al. (2015) argue that this is due to permanent but inefficient replisome blockage at *Ter* rather than transient pausing while Tus dissociates. An answer should be sought to why such a system would have evolved to work only roughly half of the time.

There is developing skepticism about aspects of the textbook view of dynamics of the *E. coli* replisome *in vivo*. The prevailing model depicts perfectly coordinated, simultaneous leading and lagging strand DNA synthesis by a stable replisome (discussed in Lewis et al. 2016). Such a deterministic model violates fundamental chemical principles (van Oijen and Dixon, 2015), not to mention the pragmatism of evolution, and it has been challenged by three recent single-molecule studies that uncover alternate pathways. The first two studies demonstrate facile exchange between complete replicase units at the fork and in solution, on the seconds timescale, both *in vivo* (Beattie et al. 2017) and *in vitro* (Lewis et al. 2017). The third study (Graham et al. 2017) suggests that even under conditions with no free polymerases in solution, the DnaB helicase can transiently uncouple and proceed more slowly ahead of the replicase at the apex of the replication fork. Although further work is necessary to fully integrate these new findings with our study of the fork rate dependence of replisome stalling at Tus–*Ter* sites (Elshenawy et al. 2015), they do not affect our conclusions.

Acknowledgements

We thank Dr. Zhi-Qiang Xu for reagents and for sharing unpublished data.

Disclosure statement

The authors report no conflicts of interest.

Funding

Funding for this work has been provided by the Australian Research Council (DP150100956) (to NED), by King Abdullah University of Science and Technology through core funding to (S.M.H.) and a Competitive Research Award (CRG5) (to S.M.H. and NED); and by a VICI grant from the Netherlands Organization for Scientific Research and an ERC Consolidator Grant (DynGenome, no 312221) from the European Research Council (both to N.H.D.).

ORCID

Bojk A. Berghuis http://orcid.org/0000-0002-7797-0553
Nicholas E. Dixon http://orcid.org/0000-0002-5958-6945
Samir M. Hamdan http://orcid.org/0000-0001-5192-1852
Nynke H. Dekker http://orcid.org/0000-0003-4029-0973

References

Bastia D, Zzaman S, Krings G, Saxena M, Peng X, Greenberg MM. 2008. Replication termination mechanism as revealed by Tus-mediated polar arrest of a sliding helicase. Proc Natl Acad Sci USA. 105:12831–12836.

Beattie TR, Kapadia N, Nicolas E, Uphoff S, Wollman AJ, Leake MC, Reyes-Lamothe R. 2017. Frequent exchange of the DNA polymerase during bacterial chromosome replication. eLife. 6:e21763.

Benkovic SJ, Valentine AM, Salinas F. 2001. Replisome-mediated DNA replication. Annu Rev Biochem. 70:181–208.

Berghuis BA, Dulin D, Xu ZQ, van Laar T, Cross B, Janissen R, Jergic S, Dixon NE, Depken M, Dekker NH. 2015. Strand separation establishes a sustained lock at the Tus–*Ter* replication fork barrier. Nat Chem Biol. 11:579–585.

Coskun-Ari FF, Skokotas A, Moe GR, Hill TM. 1994. Biophysical characteristics of Tus, the replication arrest protein of *Escherichia coli*. J Biol Chem. 269:4027–4034.

Duggin IG, Bell SD. 2009. Termination structures in the *Escherichia coli* chromosome replication fork trap. J Mol Biol. 387:532–539.

Elshenawy MM, Jergic S, Xu ZQ, Sobhy MA, Takahashi M, Oakley AJ, Dixon NE, Hamdan SM. 2015. Replisome speed determines the efficiency of the Tus-Ter replication termination barrier. Nature. 525:394–398.

Graham JE, Marians KJ, Kowalczykowski SC. 2017. Independent and stochastic action of DNA polymerases in the replisome. Cell. 169:1201–1213.

Hamdan SM, Loparo JJ, Takahashi M, Richardson CC, van Oijen AM. 2009. Dynamics of DNA replication loops reveal temporal control of lagging-strand synthesis. Nature. 457:336–339.

Hamdan SM, Richardson CC. 2009. Motors, switches, and contacts in the replisome. Annu Rev Biochem. 78:205–243.

Hidaka M, Kobayashi T, Takenaka S, Takeya H, Horiuchi T. 1989. Purification of a DNA replication terminus (*ter*) site-binding protein in *Escherichia coli* and identification of the structural gene. J Biol Chem. 264:21031–21037.

Hill TM. 1992. Arrest of bacterial DNA replication. Annu Rev Microbiol. 46:603–633.

Hill TM. 1996. Features of the chromosomal terminus region. In Neidhardt FC editor. Escherichia coli and Salmonella: cellular and molecular biology. 2nd ed., vol. 2. Washington, D.C.: American Society for Microbiology; p. 1602–1614.

Hill TM, Henson JM, Kuempel PL. 1987. The terminus region of the *E. coli* chromosome contains two separate loci that

exhibit polar inhibition of replication. Proc Natl Acad Sci USA. 84:1754–1758.

Hill TM, Marians KJ. 1990. *Escherichia coli* Tus protein acts to arrest the progression of DNA replication forks *in vitro*. Proc Natl Acad Sci USA. 87:2481–2485.

Johnson A, O'Donnell M. 2005. Cellular DNA replicases: components and dynamics at the replication fork. Annu Rev Biochem. 74:283–315.

Kamada K, Horiuchi T, Ohsumi K, Shimamoto N, Morikawa K. 1996. Structure of a replication-terminator protein complexed with DNA. Nature. 383:598–603.

Khatri GS, MacAllister T, Sista PR, Bastia D. 1989. The replication terminator protein of *E. coli* is a DNA sequence-specific contra-helicase. Cell. 59:667–674.

Lee JY, Finkelstein IJ, Arciszewska LK, Sherratt DJ, Greene EC. 2014. Single-molecule imaging of FtsK translocation reveals mechanistic features of protein–protein collisions on DNA. Mol Cell. 54:832–843.

Lewis JS, Jergic S, Dixon NE. 2016. The *E. coli* DNA replication fork. Enzymes. 39:31–88.

Lewis JS, Spenkelink LM, Jergic S, Wood EA, Monachino E, Horan NP, Duderstadt KE, Cox MM, Robinson A, Dixon NE, et al. 2017. Single-molecule visualization of fast polymerase turnover in the bacterial replisome. eLife. 6:e23932.

Mulcair MD, Schaeffer PM, Oakley AJ, Cross HF, Neylon C, Hill TM, Dixon NE. 2006. A molecular mousetrap determines polarity of termination of DNA replication in *E. coli*. Cell. 125:1309–1319.

Mulugu S, Potnis A, Shamsuzzaman, Taylor J, Alexander K, Bastia D. 2001. Mechanism of termination of DNA replication of *Escherichia coli* involves helicase–contrahelicase interaction. Proc Natl Acad Sci USA. 98:9569–9574.

Neylon C, Kralicek AV, Hill TM, Dixon NE. 2005. Replication termination in *Escherichia coli*: structure and antihelicase activity of the Tus-Ter complex. Microbiol Mol Biol Rev. 69:501–526.

Pandey M, Elshenawy MM, Jergic S, Takahashi M, Dixon NE, Hamdan SM, Patel SS. 2015. Two mechanisms coordinate replication termination by the *Escherichia coli* Tus-Ter complex. Nucleic Acids Res. 43:5924–5935.

Sahoo T, Mohanty BK, Lobert M, Manna AC, Bastia D. 1995. The contrahelicase activities of the replication terminator proteins of *Escherichia coli* and *Bacillus subtilis* are helicase-specific and impede both helicase translocation and authentic DNA unwinding. J Biol Chem. 270:29138–29144.

Valjavec-Gratian M, Henderson TA, Hill TM. 2005. Tus-mediated arrest of DNA replication in *Escherichia coli* is modulated by DNA supercoiling. Mol Microbiol. 58:758–773.

van Oijen AM, Dixon NE. 2015. Probing molecular choreography through single-molecule biochemistry. Nat Struct Mol Biol. 22:948–952.